Candidate stem cell isolation and transplantation in Hexacorallia

Shani Talice
Ben Gurion University of the Negev
Shany Barkan
Ben Gurion University of the Negev
Grace Snyder
University of Miami
Aner Ottolenghi
Ben Gurion University of the Negev
Shir Eliachar
Ben Gurion University of the Negev
Ronit Ben-Romano
Ben Gurion University of the Negev
Shelly Oisher
Ben Gurion University of the Negev
Ton Sharoni
The Hebrew University of Jerusalem
Magda Lewandowska
The Hebrew University of Jerusalem
Eliya Sultan
Ben Gurion University of the Negev
Oron Goldstein
Ben Gurion University of the Negev
Reuven Aharoni
The Hebrew University of Jerusalem
Uzi Hadad
Ben Gurion University of the Negev
Claytus Davis
Ben Gurion University of the Negev
Yehu Moran
The Hebrew University of Jerusalem https://orcid.org/0000-0001-9928-9294
Orly Gershoni-Yahalom
Ben Gurion University of the Negev
Nikki Traylor-Knowles

University of Miami

Benyamin Rosental (rosentab@post.bgu.ac.il)

Ben Gurion University of the Negev

Biological Sciences - Article

Keywords:

Posted Date: October 7th, 2022

DOI: https://doi.org/10.21203/rs.3.rs-2137324/v1

Abstract

Stem cells are the base for cell therapy due to their ability to self-renew, differentiate into other cell types, and live throughout the life of an organism. The initial cell therapy was bone marrow transplantation; bone marrow that contains haematopoietic stem cells is transferred from a healthy donor into a sick recipient to transfer the healthy genotype[1,2]. Stem cell therapy approach may be possible in corals, where there is genotypic variation in heat tolerance that influences survival during increased water temperatures[3–5]. However, we first need the ability to reliably isolate and transplant stem cells in Hexacorallia, which includes stony corals and sea anemones[6]. In this work, we used the sea anemone *Nematostella vectensis* as our model for candidate stem cell transplantation, as it is the only hexacorallian species that has fluorescent-tagged transgenic strains[7]. We established cell transplantation to show that there are cell populations exhibiting the functional characteristics of stem cells. We showed that a subpopulation of cells from *N. vectensis* can be transplanted from donor to recipient, are long-lived and self-renewing, can proliferate and differentiate, can integrate into the recipient, and rescue recipient animals treated with lethal doses of a chemotherapeutic agent. Lastly, we showed that this subpopulation can be enriched by sorting, using species non-specific cell markers and that similar subpopulations of cells can be isolated from other hexacorallians, including stony corals. This lays a foundation for the possibility of stem cell-based therapy in species of Hexacorallia.

Full Text

Stem cells are long-lived, self-renewing cell populations that differentiate into various cell types of the body throughout an organism's life. In medicine, cell and gene therapy are founded on the ability to transplant stem cells from a healthy donor or after corrective gene manipulation to a sick recipient. The integration and activity of the self-perpetuating population of healthy cells are the basis for the patient's therapy[8–13]. Historically, stem cell manipulation and transplantation formed the foundation for understanding the development and maintenance of tissue and organ function, especially the hematopoietic and immune systems[9,12,13].

Stem cell initial identification begins with satisfying a set of defined functional properties when transferred from donor to recipient: ( ) cell integration and proliferation in recipient tissues, ( ) persistence of donor genotype and phenotype in the recipient, ( ) rescue of damaged animals and/or tissues, ( ) longevity of those cells, (V) the ability to differentiate into other cell types, and ( ) the ability to be enriched by isolation of subpopulations with the above stem cell properties[2,13,14]. Once characterized, stem cells may be isolated on the basis of the markers they express. For transplantation-based therapy, these properties are defined at the functional level; there are no requirements that the subpopulation be a single cell type[1,2,15]. This was exemplified in the first instance of stem cell therapy in humans, where bone marrow transplantation preceded the isolation of the "pure" haemotopoietic stem cell population[16,17]. This formed the foundation for the isolation and identification of hematopoietic stem cells.

Using the same principles of this pioneering work, stem cell transplantation was later applied to invertebrates, including Tunicates, Planarians, and Hydrozoans[14,18–23]. However, in other invertebrates, including Hexacorallia (Phylum: Cnidaria), stem cell isolation and transplantation in adult animals have not been established, even though there are indications that progenitor/stem cells are present[24–28].

There is a need to establish stem cell transplantation methods in hexacorallians because of anthropogenic climate change, mainly driven by increasing water temperatures, is quickly destroying the world's coral reefs[29,30]. There is genotypic variation in the coral response to heat stress. Some genotypes of the same species are more thermally resilient than others[31–37]. Thus, stem cell transplantation has the potential to be a therapeutic approach in corals, where transplantation could be used to reestablish health or help confer resistance to heat stress. For this to become feasible stem cell transplantation in hexacorallian models needs to be established.

In this report, we describe a classic functional approach toward stem cell transplantation in a hexacorallian model, the sea anemone *Nematostella vectensis*. We describe the transplantation of cells meeting the six described functional properties of stem cells. We also isolated a candidate stem cell population using species non-specific markers. By using this generalized approach, stem cell transplantation-based therapy can be applied to other hexacorallians, including stony corals.

Cell transplantation

First, we determined whether we could transfer cells between adult animals. Donor animals were transgenic, ubiquitously expressing the mCherry reporter from a promoter of a housekeeping gene (*TBP::mCherry*)[7]. Recipient animals were wild-type (WT) and were pretreated with a sublethal dose of Mitomycin-C (MITC) (30 μM; Fig. S1b) to provide donor cells with a competitive advantage after transplantation. A cell suspension of approximately 100,000 donor cells was injected into recipient animals (Fig. S1a). The recipient animals were then monitored for up to two months by fluorescent microscopy. Following the monitoring, the recipients were then prepared for flow cytometry and PCR analysis (Fig. 1a).

We observed an increase in the number of animals containing visible mCherry over time (Fig. 1c). Four days after transplantation, the majority of recipient animals (90%) did not exhibit any visible mCherry but by 20 days most of the animals (90%) became mCherry-positive (Fig. 1c). The 90% of recipient animals that were mCherry-positive at 20 days remained positive until termination of the experiments two months after transplantation. The mCherry signal observed was broadly distributed in different tissues in the recipient animals (Fig. 1b). Flow cytometry at the termination of the experiment provided a quantitative measure of chimerism. 20% - 55% of cells from recipient animals exhibited an mCherry signal (mCherry-positive cells) (Fig. 1d-e). In contrast, in MITC-treated non-transplanted animals, less than 10% of cells scored positive, which was comparable to the 13% of the basal levels of

autofluorescence in the mCherry channel in cells from untreated WT animals (Fig. 1e, negative control). The persistence of donor genetic material in the recipient animals was confirmed by PCR amplification of the donor mCherry DNA, which was observed in transplanted animals, but not in non-transplanted animals (Fig. 1F, S1c).

Donor mCherry-positive cells showed proliferation following their transplantation. Dissociation of an animal yields 1-2 million cells; the recipient animals contained approximately 200,000-1,000,000 donor cells at the termination of the experiment; however, only 100,000 donor cells were transplanted initially in each animal (Fig. 1e-f). This suggests that some donor cells survived and proliferated at least several cycles in the recipients.

Candidate stem cell integration and longevity

Stem cell integration can rescue animals from death by integrating into damaged tissues. To test this, we treated recipient animals with lethal doses of MITC and then transplanted cells from healthy untreated donors. Transplantation significantly reduced the death of the recipient animals compared to MITC-treated, non-transplanted animals (Fig. 2a-b). This indicates that the donor cells are able to functionally integrate into the host and complement missing activity, thus rescuing the animal from death.

We next assessed the longevity and persistence of transplanted cells by serial transplantation. mCherry-expressing donor cells were injected into sublethal MITC-treated recipients. After 6-8 weeks recipient animals were dissociated and mCherry-positive cells were isolated by FACS. mCherry-positive cells were then transplanted into new MITC pre-treated WT recipients (Fig. 2c). The WT animals were then monitored weekly by microscopy for mCherry fluorescence for 6 weeks (Fig. S2). The fraction of live animals that showed a clear mCherry signal increased steadily over 6 weeks of observation (Fig. S3). At week 6, more than 80% of the transplanted animals presented a mCherry signal (Fig. 2d). These data indicate that the transplanted donor cells are capable of at least two rounds of transplantation and re-integration.

Together these data suggest that stem cell populations are present in *N. vectensis* and persist within recipient tissues alongside the endogenous cells following transplantation. If the signal were due to donor material uptake, then it would be expected that the mCherry signal would be highest just after transplantation and then decrease as donor material is metabolized. However, we observed the opposite (Fig. 1c, 2d, S3). The mCherry signal was attenuated immediately after transplantation and then slowly became stronger over time. These data suggest that initially many transplanted cells die, but a subpopulation survives, recovers, and divides to re-establish the mCherry signal. Thus, a majority of the fundamental stem cell properties are exhibited: ( ) cell integration and proliferation in recipient tissue, ( ) persistence of donor genotype in the recipient, ( ) rescue of damaged animals/tissues, and ( ) longevity (Fig. 1, 2, S1c, S2, S3).

Candidate stem cell isolation

We then established a strategy to isolate a population of cells that were an enriched source of putative stem cells. In the colonial tunicate, *Botryllus schlosseri*, such a subpopulation of cells was previously isolated by FACS based on increased ALDH activity and decreased granularity[14]. Increased ALDH activity has also been used to select mammalian hematopoietic stem cells[38]. We hypothesized that increased ALDH activity and low granularity might be characteristic of stem cells in Hexacorallia. To test this, WT animals were incubated with EdU for four hours and then dissociated and sorted by FACS into two cell populations, a high ALDH activity/low granularity (ALDH-high) and a low ALDH activity/ high granularity (ALDH-low) (Fig. 3a-b). The amount of EdU incorporated into cells was assessed by flow cytometry. In all animals tested the ALDH-high cells had significantly higher amounts of EdU incorporation than the ALDH-low cells (Fig. 3c). Microscopy indicated that the ALDH-high cells were fairly uniform in appearance; the large majority of cells were hemoblast-like, small with scant cytoplasm. In contrast, the ALDH-low cells were, on average, larger and much more diverse in morphology (Fig. 3b).

We then characterized the putative stem cell-enriched subpopulation in transplantation assays. mCherry-positive donor animals were dissociated and sorted by FACS to generate ALDH-high and ALDH-negative subpopulations. Approximately 10,000 cells from each of these were then transplanted into MITC-treated WT recipients (Fig. 3a). Fluorescent and confocal microscopy confirmed a clear mCherry signal in recipient animals over two months following the transplantation of ALDH-high donor cells (Fig. 3e). In contrast, recipients after the transplantation of ALDH-low donor cells showed a mCherry signal after transplantation that faded over time (Fig. 3d-e).

The relative contributions of donor-derived ALDH-high vs ALDH-low cells to recipient animals were assessed by flow cytometry with gating for mCherry fluorescent cells three weeks after transplantation. Under the same conditions, ALDH-high donor-derived cells constituted up to 8% of the recipient. ALDH-low donor-derived cells contributed less than 3% to recipients in all instances (Fig. S4a). We observed a distinct cell population of donor-derived mCherry-positive cells in recipient animals transplanted with ALDH-high cells. In ALDH-low recipient animals, the mCherry positive cell population was significantly smaller and not as distinct, even when comparing a close percentage of chimerism of the lowest animal of ALDH-high to highest in ALDH-low (Fig S4a; lower panels).

This initial analysis was then repeated over an extended time course of two months. Fluorescent microscopy analysis suggested that while both the transplanted cell populations of ALDH-high and ALDH-low integrated, with time the ALDH-high persists, while the ALDH-low recipient mCherry-positive animals decline after 40 days (Fig. 3e). Moreover, comparing the 3-weeks experiment to the 2-months experiment suggested that the number of donor-derived cells following transplantation of ALDH-high cells increased (reaching 25%; average 12%) while the representation of ALDH-low donor-derived cells in recipients decreased to the non-transplant control levels (Fig. 3f). The presence of donor DNA was

measured by PCR four weeks after transplantation of ALDH-high and ALDH-low cells into recipients (Fig. S4b). The PCR data were consistent with the flow cytometry results. The data indicate that the isolation of *N. vectensis* ALDH-high cells enriches for a functional candidate stem cell population.

Candidate stem cell differentiation

One of the fundamental properties of stem cells is differentiation into other cell types. To assess this, we compared the morphology of three populations of cells: ALDH-high cells before transplantation, donor-derived mCherry-positive cells from recipients two months after transplantation of ALDH-high cells, and total cells (Fig. 4a). The ALDH-high donor cells were small, 2-4 microns in diameter, round cells that looked like hemoblasts (Fig. 4a, left panel). Two months after transplantation, many of the cells in the recipient that were derived from these donor cells had changed morphology (Fig. 4a, center panel). Some cells retained the hemoblast morphology, but others were granular and larger (up to 20 microns in diameter) and some had the distinctive appearance of nematocytes (Fig. 4a, center image). In general, after transplantation, the donor-derived cells (Fig. 4a, center image) resembled the total cells (Fig. 4a, right image).

To validate our morphological observations, we used an unbiased approach for assessing differentiation, a machine learning algorithm operating on microscope images of fields of cells from different cell populations. The procedure successfully identified cells (Fig. 4b) and assessed variation in cell area and shape (Fig. 4c-d). Confirming our visual impression, these data indicated that after two months the donor-derived mCherry-expressing cells more closely resembled the total cell population (Fig. 4d, right) than the source cells (Fig. 4c, 4d left). We conclude that some of the ALDH-high donor cells or their progeny differentiated into different cell types following transplantation into recipients.

Generalization of the isolation strategy

The sort parameters used to isolate the stem cell-enriched subpopulation from *N. vectensis* were, by design, species non-specific and had previously been shown to work in very distantly related metazoans[14,38]. Given that one of the long-term goals of this research is to apply the transplantation approach to other hexacorallians, including stony corals, we tested whether these parameters could be used similarly to isolate a subpopulation of cells from two other hexacorallians, the symbiont-containing sea anemone *Exaiptasia diaphana,* and the stony coral *Pocillopora damicornis*. While the cell populations were somewhat different, a subpopulation of cells that were ALDH-high/granularity low could be isolated from all three species (Fig. 4e), suggesting that our approach may work across a diverse variety of hexacorallian species.

Discussion

As mentioned previously, stem cells can be defined by a set of functional properties when transferred from donor to recipient. These properties were addressed in our transplantation experiments in *N. vectensis*. (I) The ability to integrate and proliferate was demonstrated by the mCherry signal over time (Fig. 1c, 2d), and in the number of donor-derived cells after transplantation (Fig. 1d-e). The PCR analysis (Fig. 1f, S1c) and serial transplantation experiments (Fig. 2c-d) showed (II) the ability of those cells to retain their genotype/phenotype in a recipient animal. (III) The rescuing ability of these candidate stem cells is demonstrated by survival tests (Fig. 2a-b). The serial transplantation experiments showed (IV) the longevity of those cells (Fig. 2c-d). To show stem cell enrichment, we isolated a subpopulation with high ALDH activity and low granularity by FACS. First, the proliferation ability of those cells was shown by the EdU incorporation (Fig. 3c). Then we showed their ability to integrate and proliferate (Fig. 3d-f, S4a). The persistence of the ALDH-high cells was shown by PCR analysis (Fig. S4b) and (V) the ability to differentiate was shown by cell morphology change (Fig. 4a-d). These findings demonstrate that there is a candidate stem cell subpopulation that can be enriched and isolated in *N. vectensis* (VI).

As coral reef habitats worldwide are under threat[29,30], these findings can push us closer to applying stem cell therapy in corals. The enrichment for stem cell subpopulations was done by using a species non-specific marker (ALDEFLUOR), it can be used in other hexacorallian species, including stony corals, which constitute the foundation of coral reefs (Fig. 4e). This opens the possibility for stem cell therapy for corals, either syngeneic with gene therapy or allogeneic from a resilient donor to a sensitive recipient. Moreover, these findings may help researchers to understand how the developmental programs that construct and regenerate the organism function and change during evolution.

We show here on the functional level the existence of a stem cell-like population in Hexacorallia including the ability to isolate and enrich them. Although there is data supporting the existence of a stem cell population in Hexacorallia, including *N. vectensis*[24,27,28], it is conceivable that, in their absence, progenitor cells are generated by dedifferentiation. Even if this is the case, such cells represent a transient population that exhibits a higher transplantability potential than other cells, opening up the potential for cell-based therapy, despite not being “true” stem cells.

It is important to note, that while this is an important step, there are many challenges to overcome for making cell therapy possible in corals. While the flow cytometry analysis indicates a high ALDH activity and low granularity cell population in stony corals, future experiments using high throughput sequencing and transplantation assays will show if these are similarly enriched for a functional stem/progenitor cell population. Here we show transplantation to a solitary polyp species and we acknowledge that there is still the need to show that transplanted cells can migrate within a colonial species. Previous studies in medusozoans have shown cell transfer between polyps[20,39]. Within corals at a colony level, genetic chimerism after fusion can occur[4,5,40]. The chimerism observed raises questions about allorecognition in Hexacorallia[41,42], which could be a challenge for the use of stem cell therapy in the future. However, there are also examples of chimerism and natural transplantations in corals, suggesting that allorecognition can be overcome[43–45].

While there are examples of genetic polymorphism affecting differently the heat resilience of individuals of the same species[3,32,33,36], the specific genes which enable heat tolerance are largely unknown. For stem cell-based gene-therapy to become feasible, genes of resilience need to be found as well as genetic manipulation abilities[46].

In conclusion, we show here that within adult *N. vectensis* there are subpopulations of cells that have the functional characteristics of stem cells. We isolated a subpopulation of cells, using species non-specific markers, that are enriched for these candidate stem cells. This research lays the foundation for important basic and applied research in stem cell biology and regeneration mechanisms in Hexacorallia. Moreover, it opens the possibility for research and development of cell therapy in corals using gene therapy or direct transplantation from stress-resilient animals to sensitive corals.

Materials And Methods

Animal husbandry

The *N. vectensis* strains used were highly inbred WT and a transgenic line, ubiquitously expressing mCherry (TBP::mCherry)[7]. *N. vectensis* were grown in the dark, in plastic dishes of 14 ppt artificial seawater (ASW), pH 8-8.6, and 18 °C in an incubator. Animals were housed in the mariculture room at the Regenerative Medicine and Stem Cell Research Center, Ben Gurion University (Approved by the Israel ministry of agriculture and university biosafety committee).

Mitomycin-C treatment

Before the Mitomycin-C (MITC) chemotherapy, the animals were not fed for at least three days. Then the MITC was diluted in the *N. vectensis* water (14 ppt, pH 8-8.6) to the desired concentration. In this mix, the treated animals were incubated for ~13 h, followed by a series of five washes and an additional wash the day after, to make sure the MITC will no longer be in our experimental system. As a result, three days after the MITC treatment, the animals were used for transplantation.

The lethal and sublethal doses of MITC were also tested in this study and revealed they are about 45 µM and below, and 60 µM and above, respectively (Fig. S1b). Therefore, for the survival experiments, we used lethal doses of MITC and for the regular transplantation experiment, we used sublethal doses.

Cell dissociation

Firstly, the cell dissociation process was done mechanically by using a sterile scalpel and filtered through a 100 µm strainer where the cells were dissociated and pushed with a sterile syringe piston, then this process was repeated with a 40 µm strainer.

Through the whole cell dissociation process from *N. vectensis* the cell media that was used for the *ex-vivo* cells, was composed of L-15 with 1.42× PBS molarity (by diluting Ca, Mg free 10× PBS in the solution), 2% of FBS, and 10 mM of HEPES.

Transplantation process

Before cell transplantation the animals were treated with 0.05 M of $MgCl_2$ in *N. vectensis* water for ~20 minutes, resulting in paralysis. Then, we transferred them into a 10 cm petri dish with a piece of plasticine (to ease the injection process) and *N. vectensis* water with 0.05 M of $MgCl_2$.

The transplantation system is composed of a stereo microscope (Stemi 305, stand K LAB, Zeiss), a capillary needle (Borosilicate glass with filament; O.D.: 1.2 mm; I.D.:0.94 mm; Sutter), and a micromanipulator system (InjectMan® 4; Eppendorf), connected to an oil injection system (CellTram® 4r Oil, Eppendorf) (Fig. S1a).

Using this system, we loaded the cells (for each animal separately) into the capillary (~10 µl) from a paraffin paper. Then, the animal is loaded into the transplantation system, and we transplant the cells into the physa and/or the mesenteries area. To end the $MgCl_2$ paralysis effect we wash the animals 6 times before transferring them into a properly labeled 6-well plate (one animal/well) for further follow-up.

Cell transplantation experiments

The cell transplantation experiment began with the treatment of sublethal doses of MITC in WT animals (as previously described). On the day of the cell transplantation, the cells from transgenic *TBP::mCherry* animals (not fed for at least 3 days) were dissociated. Then the cells were centrifuged for transplantation (500 x g for 10 min.). Resuspended in ~150 µl, and ~10 µl of cell solution were transplanted into each animal in the “Transplanted” animal group. Whereas the “Non-transplanted” animal group did not receive transplantation but did receive the MITC treatment and the same injection trauma as the “Transplanted” animal group. At the end of the experiment (~3-8 weeks after transplantation), animals were sacrificed, and the presence of mCherry was tested by PCR, qPCR, and presence of fluorescence by flow cytometry analysis (CytoFLEX-S, Beckman Coulter) (Fig. 1a).

For the survival assays, the same cell transplantation experiments were conducted, with lethal doses of MITC.

Serial cell transplantation experiments

The serial cell transplantation experiment began with the same process as the cell transplantation experiments, until the end of the transplantation. The cell dissociation process from the transplanted animals was done, flowed by cell sorting using the FACS (Sony-MA 900 or BD-Aria III) to sort out the mCherry-positive cells. The addition of ROCK inhibitor (Y-27632 dihydrochloride; C# 1254/1; Tocris) was done to reduce cell death.

These transplanted mCherry-positive cells were then transplanted again into new WT animals that were also treated with MITC, which were divided into two groups: I) “Transplanted” – transplanted with mCherry-positive cells from a transplanted animal; II) “Non-transplanted” – have the same MITC treatment as the “Transplanted” animal group, as well as the same injection trauma.

Transplantation of ALDH-positive cell population

As described above, the cell dissociation process from transgenic *TBP::mCherry* animals was conducted with the addition of ALDEFLUOR stain to detect ALDH activity (ALDEFLUOR^{TM} kit; C# 01700; STEMCELL^{TM}) and ROCK inhibitor (Y-27632 dihydrochloride; C# 1254/1; Tocris). Flowed by FACS sorting for ALDH-positive/side scatter-low and ALDH-negative/side scatter high cell populations. These cell populations were then transplanted into the corresponding animal groups, labeled as “ALDH-positive” and “ALDH-negative”, respectively. In addition, there was another control group labeled as “Non-transplanted” with the same MITC treatment and the same injection trauma.

Microscopy

For whole animal analysis, after cell transplantation, the animals were incubated in a 6-well plate (animal/well) in *N. vectensis* water and were observed for further follow-up by a fluorescent stereo microscope (Leica M205 FA), or confocal microscope (LSM900; Zeiss). For cellular analysis, the cells were sorted by FACS into cell populations in this research including ALDH-positive, ALDH-negative, and total cell populations. mCherry-positive cells were sorted following the end of transplantation experiments. The cells were in *N. vectensis* cell media and loaded into a micro-well slide for observation by a confocal microscope (LSM900; Zeiss). The images were analyzed by ZEN 3.3 blue edition software.

Machine learning analysis for cell morphology

After an experiment of transplantation of ALDH-positive cells, FACS sorting was done on cells from a pool of the transplanted animals for different cell populations, including ALDH-positive cells, mCherry-positive cells (after transplantation), and total cells (all the living cells in the analysis).

The different cell populations were resuspended in *N. vectensis* cell media and loaded into a microplate (3 wells/cell population) for confocal-brightfield imaging (LSM900; Zeiss). The analysis of the cell morphology in the resulting confocal images was done by image segmentation. In order to segment cell boundaries in brightfield images, we used the Zeiss Zen Blue 3.5 Intellesis Trainable Segmentation tool. A Deep 64 Features model was trained on 10-12 segments of Object and Background pixels. Model training was repeated until a sufficient level of segmentation was achieved. Cells in proximity that the trained model could not separate were separated manually. The formula for circularity was:

$$\sqrt{\frac{4 \cdot Area}{\pi \cdot FeretMax^2}}$$

Flow cytometry analysis

For cell analysis by flow cytometry from transplanted animals, the animals were used without the head, due to some auto-fluorescence of some of the animals in their “corona” area. The native fluorescent

protein NvFP-7R, a DsRed homolog expressed in *N. vectensis* polyps, is likely the reason for the basal autofluorescence[47]. The flow cytometry analysis was done with the CytoFlex (CytoFLEX-S, Beckman Coulter) flow cytometer, data was analyzed by CytExpert software (version 2.4.0.28). This method was used to detect the mCherry-positive cells after cell transplantation. The first gating was based on forward-scatter against side-scatter to detect cells vs debris in the analyzed sample. The second gate was done to detect the mCherry-positive cells in a plot of the mCherry against the PE-Cy7 channel. This was done to be able to detect the auto-florescence (diagonal) vs the specific mCherry (above the diagonal) since both colors are excited with the same laser but emit in a different wavelength. As was previously done in flow cytometry analysis of fluorescent animals[22,48].

PCR

For the PCR analysis, the animals underwent a shock freeze with liquid nitrogen to end the cell transplantation experiment. Then, the DNA was isolated from each animal separately for the PCR analysis with a DNA purification kit (Genomic Mini AX Tissue Spin; C# 056-100S; A&A Biotechnology). Eventually, the PCR process was conducted to amplify the mCherry gene (forward primer: ACATGGCCATCATCAAGGAGTTCA; reverse primer: TCGGCGCGTTCGTACTGT; final product=643 bp) and, as a control, a housekeeping gene of *N. vectensis* was also amplified (HKG4; forward primer: CTCAAGGCTGAGGCTGTGGAC; reverse primer: CTTTGGGTAATCTGTGAACTTGACCACT; final product=381 bp), with a PCR mix of PCRBIO HS Taq Mix Red (C# PB10.23-02; PCRBIOSYSTEMS). The PCR program was set according to the enzyme mix protocol. The gel PCRBIO Ladder II (250bp - 10kb; C#PB40.12-01), was used.

qPCR

For the qPCR analysis, the animals underwent a shock freeze with liquid nitrogen to end the cell transplantation experiment. DNA isolation of the experimental animals was done with a DNA purification kit (Genomic Mini AX Tissue Spin; C# 056-100S; A&A Biotechnology). mCherry was amplified (forward primer: GACATCCTGTCCCCTCAGTTC; reverse primer: GGGGAAGGACAGCTTCAAGTA) along with control housekeeping gene (HKG4; forward primer: GCTCAAACCTGGTCTTCTACCTATG; reverse primer: GCGATGGGTGCAATGACA) The qPCR mix in use was qPCRBIO SyGreen Blue Mix Lo-ROX (C# PB20.15-05; PCRBIOSYSTEMS) and amplification program was set according to enzyme mix protocol. The instrument used was QuantStudio ™ 5 System.

Declarations

Funding

BR has received funding from European Research Council (ERC) under the European Union's Horizon 2020 research and innovation program under grant agreement No. 948476. NTK and BR were supported by the Revive and Restore grant number: 2020-011. NTK and BR were supported by NSF-BSF Integrative and Organismal Systems (IOS) Grant: BSF grant number 2019647, NSF grant number 1951826. BR would

like to thank Alex and Ann Lauterbach for funding the Comparative and Evolutionary Immunology Laboratory. The work of BR was supported by Israel Science Foundation (ISF) numbers: 1416/19 and 2841/19. BR has received funding from an HFSP grant (RGY0085/2019). Part of this work was supported by ERC consolidator grant 863809 under Horizon 2020 to YM.

References

1. Thomas, E. D., Lochte, H. L., Lu, W. C. & Ferrebee, J. W. Intravenous Infusion of Bone Marrow in Patients Receiving Radiation and Chemotherapy. *New England Journal of Medicine* **257**, 491–496 (1957).

2. Till, J. E. & McCulloch, E. A. A Direct Measurement of the Radiation Sensitivity of Normal Mouse Bone Marrow Cells. *Radiat Res* **178**, AV3–AV7 (1961).

3. Morikawa, M. K., Palumbi, S. R., Baker, A. C., Kaufman, L. & Knowlton, N. Using naturally occurring climate resilient corals to construct bleaching-resistant nurseries. *Proc Natl Acad Sci U S A* **116**, 10586–10591 (2019).

4. Oury, N., Gélin, P. & Magalon, H. Together stronger: Intracolonial genetic variability occurrence in Pocillopora corals suggests potential benefits. *Ecol Evol* **10**, 5208–5218 (2020).

5. Schweinsberg, M., Weiss, L. C., Striewski, S., Tollrian, R. & Lampert, K. P. More than one genotype: how common is intracolonial genetic variability in scleractinian corals? *Mol Ecol* **24**, 2673–2685 (2015).

6. Zapata, F. *et al.* Phylogenomic Analyses Support Traditional Relationships within Cnidaria. *PLoS One* **10**, e0139068 (2015).

7. Admoni, Y., Kozlovski, I., Lewandowska, M. & Moran, Y. TATA Binding Protein (TBP) Promoter Drives Ubiquitous Expression of Marker Transgene in the Adult Sea Anemone Nematostella vectensis. *Genes (Basel)* **11**, 1–11 (2020).

8. Bragança, J., Lopes, J. A., Mendes-Silva, L. & Santos, J. M. A. Induced pluripotent stem cells, a giant leap for mankind therapeutic applications. *World J Stem Cells* **11**, 421–430 (2019).

9. Cutler, C. & Antin, J. H. Peripheral Blood Stem Cells for Allogeneic Transplantation: A Review. *Stem Cells* **19**, 108–117 (2001).

10. Duncan, T. & Valenzuela, M. Alzheimer's disease, dementia, and stem cell therapy. *Stem Cell Res Ther* **8**, 1–9 (2017).

11. Higuchi, A. *et al.* Stem cell therapies for myocardial infarction in clinical trials: bioengineering and biomaterial aspects. *Laboratory Investigation 2017 97:10* **97**, 1167–1179 (2017).

12. Weissman, I. L. Stem Cells: Units of Development, Units of Regeneration, and Units in Evolution. *Cell* **100**, 157–168 (2000).

13. Weissman, I. L. Translating Stem and Progenitor Cell Biology to the Clinic: Barriers and Opportunities. *Science (1979)* **287**, 1442–1446 (2000).

14. Laird, D. J., de Tomaso, A. W. & Weissman, I. L. Stem cells are units of natural selection in a colonial ascidian. *Cell* **123**, 1351–1360 (2005).

15. Sabin, F. R. Preliminary Note on the Differentiation of Angioblasts and the Method by Which They Produce Blood-Vessels, Blood-Plasma, and Red Blood-Cells As Seen in the Living Chick. *Wistar Institute of Anatomy and Biology* https://profiles.nlm.nih.gov/spotlight/rr/catalog/nlm:nlmuid-101584641X87-doc (1917).

16. Baum, C. M., Weissman, I. L., Tsukamoto, A. S., Buckle, A. M. & Peault, B. Isolation of a candidate human hematopoietic stem-cell population. *Proceedings of the National Academy of Sciences* **89**, 2804–2808 (1992).

17. Spangrude, G. J. *et al.* Mouse Hematopoietic Stem Cells. *Blood* **78**, 1395–1402 (1991).

18. Gahan, J. M., Bradshaw, B., Flici, H. & Frank, U. The interstitial stem cells in Hydractinia and their role in regeneration. *Curr Opin Genet Dev* **40**, 65–73 (2016).

19. Hayashi, T., Asami, M., Higuchi, S., Shibata, N. & Agata, K. Isolation of planarian X-ray-sensitive stem cells by fluorescence-activated cell sorting. *Dev Growth Differ* **48**, 371–380 (2006).

20. Müller, W. A., Teo, R. & Frank, U. Totipotent migratory stem cells in a hydroid. *Dev Biol* **275**, 215–224 (2004).

21. Raz, A. A., Wurtzel, O. & Reddien, P. W. Planarian stem cells specify fate yet retain potency during the cell cycle. *Cell Stem Cell* **28**, 1307-1322.e5 (2021).

22. Rosental, B. *et al.* Complex mammalian-like haematopoietic system found in a colonial chordate. *Nature 2018 564:7736* **564**, 425–429 (2018).

23. Wagner, D. E., Wang, I. E. & Reddien, P. W. Clonogenic neoblasts are pluripotent adult stem cells that underlie planarian regeneration. *Science (1979)* **332**, 811–816 (2011).

24. Amiel, A. R., Foucher, K., Ferreira, S. & Röttinger, E. Synergic coordination of stem cells is required to induce a regenerative response in anthozoan cnidarians. *bioRxiv* 2019.12.31.891804 (2019) doi:10.1101/2019.12.31.891804.

25. Gold, D. A. & Jacobs, D. K. Stem cell dynamics in Cnidaria: are there unifying principles? *Dev Genes Evol* **223**, 53 (2013).

26. Lecointe, A., Domart-Coulon, I., Paris, A. & Meibom, A. Cell proliferation and migration during early development of a symbiotic scleractinian coral. *Proceedings of the Royal Society B: Biological Sciences* **283**, (2016).

27. Sebé-Pedrós, A. *et al.* Cnidarian Cell Type Diversity and Regulation Revealed by Whole-Organism Single-Cell RNA-Seq. *Cell* **173**, 1520-1534.e20 (2018).

28. Steger, J. *et al.* Single-cell transcriptomics identifies conserved regulators of neuroglandular lineages. *Cell Rep* **40**, 111370 (2022).

29. Hughes, T. P. *et al.* Global warming and recurrent mass bleaching of corals. *Nature 2017 543:7645* **543**, 373–377 (2017).

30. Mason, R. A. B., Skirving, W. J. & Dove, S. G. Integrating physiology with remote sensing to advance the prediction of coral bleaching events. *Remote Sens Environ* **246**, (2020).

31. Barshis, D. J. *et al.* Genomic basis for coral resilience to climate change. *Proc Natl Acad Sci U S A* **110**, 1387–1392 (2013).

32. Bay, R. A. & Palumbi, S. R. Multilocus Adaptation Associated with Heat Resistance in Reef-Building Corals. *Current Biology* **24**, 2952–2956 (2014).

33. Dixon, G. B. *et al.* Genomic determinants of coral heat tolerance across latitudes. *Science (1979)* **348**, 1460–1462 (2015).

34. Fine, M., Gildor, H. & Genin, A. A coral reef refuge in the Red Sea. *Glob Chang Biol* **19**, 3640–3647 (2013).

35. Grottoli, A. G., Tchernov, D. & Winters, G. Physiological and biogeochemical responses of super-corals to thermal stress from the northern gulf of Aqaba, Red Sea. *Front Mar Sci* **4**, 215 (2017).

36. Maor-Landaw, K. & Levy, O. Gene expression profiles during short-term heat stress; branching vs. massive Scleractinian corals of the Red Sea. *PeerJ* **2016**, (2016).

37. Sawall, Y. *et al.* Extensive phenotypic plasticity of a Red Sea coral over a strong latitudinal temperature gradient suggests limited acclimatization potential to warming. *Scientific Reports 2015 5:1* **5**, 1–9 (2015).

38. Storms, R. W. *et al.* Isolation of primitive human hematopoietic progenitors on the basis of aldehyde dehydrogenase activity. *Proc Natl Acad Sci U S A* **96**, 9118–9123 (1999).

39. Sanders, S. M. *et al.* CRISPR/Cas9-mediated gene knockin in the hydroid Hydractinia symbiolongicarpus. *BMC Genomics* **19**, 1–17 (2018).

40. Puill-Stephan, E., Willis, B. L., van Herwerden, L. & van Oppen, M. J. H. Chimerism in Wild Adult Populations of the Broadcast Spawning Coral Acropora millepora on the Great Barrier Reef. *PLoS One* **4**, e7751 (2009).

41. Amar, K. O., Chadwick, N. E. & Rinkevich, B. Coral kin aggregations exhibit mixed allogeneic reactions and enhanced fitness during early ontogeny. *BMC Evol Biol* **8**, 1–10 (2008).

42. Puill-Stephan, E., Willis, B. L., Abrego, D., Raina, J. B. & van Oppen, M. J. H. Allorecognition maturation in the broadcast-spawning coral Acropora millepora. *Coral Reefs* **31**, 1019–1028 (2012).

43. Huffmyer, A. S., Drury, C., Majerová, E., Lemus, J. D. & Gates, R. D. Tissue fusion and enhanced genotypic diversity support the survival of Pocillopora acuta coral recruits under thermal stress. *Coral Reefs* **40**, 447–458 (2021).

44. Rinkevich, B. Coral chimerism as an evolutionary rescue mechanism to mitigate global climate change impacts. *Glob Chang Biol* **25**, 1198–1206 (2019).

45. Vidal-Dupiol, J. *et al.* Frontloading of stress response genes enhances robustness to environmental change in chimeric corals. *BMC Biology 2022 20:1* **20**, 1–18 (2022).

46. Voolstra, C. R. *et al.* Extending the natural adaptive capacity of coral holobionts. *Nature Reviews Earth & Environment 2021 2:11* **2**, 747–762 (2021).

47. Ikmi, A. & Gibson, M. C. Identification and In Vivo Characterization of NvFP-7R, a Developmentally Regulated Red Fluorescent Protein of Nematostella vectensis. *PLoS One* **5**, (2010).

48. Rosental, B., Kozhekbaeva, Z., Fernhoff, N., Tsai, J. M. & Traylor-Knowles, N. Coral cell separation and isolation by fluorescence-activated cell sorting (FACS). *BMC Cell Biol* **18**, 1–12 (2017).

Figures

Figure 1

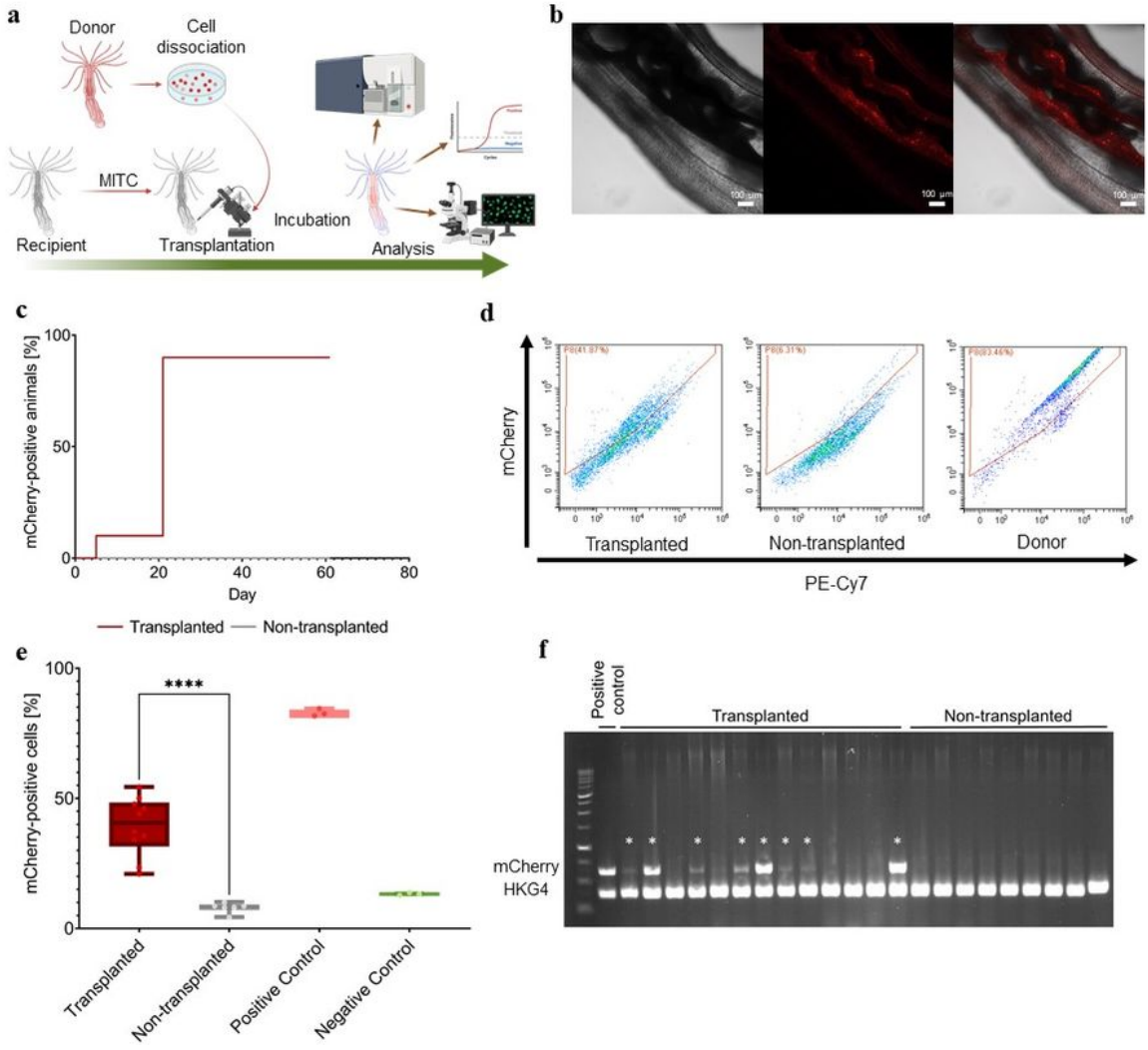

Figure 1

Cell transplantation in *N. vectensis*. (a) Experimental setting, recipient wild-type (WT) *N. vectensis* were treated with Mitomycin-C (MITC) 3 days before the transplantation. Donor animals expressing the mCherry reporter under the regulation of the housekeeping TBP promoter (transgenic *TBP::mCherry*) were then dissociated and single-cell suspensions of approximately 100,000 donor cells were transplanted by microinjection into each MITC-treated recipient animal. Donor-derived mCherry signal in the recipients

was periodically assessed by confocal/fluorescent microscopy for up to two months. At the experiment end, the donor-derived mCherry signal was assayed also by FACS and PCR. **(b)** mCherry signal in recipient animal mesentery area 7 days following transplantation of donor cells. Brightfield image - left, fluorescent mCherry image - middle, merged image - right. **(c)** Representative experiment showing percentage of recipient animals with mCherry signal. 10 transplanted and 10 non-transplanted animals that had been MITC-treated were monitored for mCherry on the days indicated. **(d-e)** Frequency of mCherry positive cells 40 days after the transplantation. 11 transplanted animals, 10 non-transplanted animals, 1 donor animal (triplicate - positive control), and 1 WT animal (triplicate - negative control) were dissociated to generate single-cell suspensions (**e**), mCherry signal was assessed by flow cytometry (median, 25th to 75th percentiles, and minimum to maximum values shown, **** - *P*= <0.0001, unpaired t-test). Representative results for a single animal in each group are shown (**d**), red gate shows the positive cut-off values against non-specific basal autofluorescence of the native protein NvFP-7R (PE-Cy7). **(f)** mCherry DNA in transplanted recipients. DNA was extracted from an individual donor/positive control (n=1), transplanted (n=12) and non-transplanted (n=9) animals at the end of the experiment. The presence of mCherry DNA was assessed by PCR amplification of a 643 bp mCherry-specific DNA sequence. Co-amplification of a 381 bp HKG4 sequence found in all the genomes, served as an internal positive control (* - individuals scored positive).

47

Figure 2

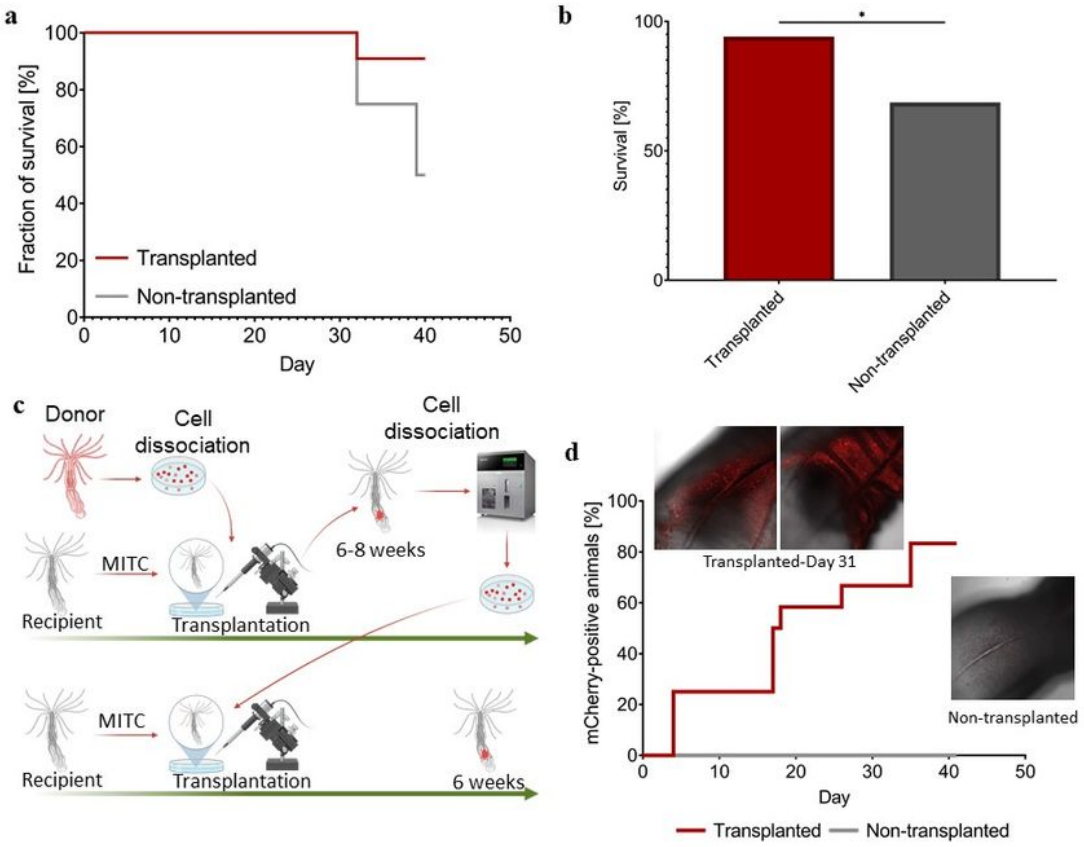

Figure 2

Recipient rescue and transplanted cell longevity. (a-b) For survival assays, non-transplanted animals were treated with a lethal dose of MITC (75 μM) and three days later injected with donor cells. Their viability was scored weekly. **(a)** Survival curve of one representative experiment of 11 transplanted and 10 non-transplanted. **(b)** Four rescue experiments were repeated to yield 34 animals in the Transplanted group and 32 in the Non-transplanted group. The fraction of surviving animals 4-8 weeks after transplantation

was calculated (* - P=0.0103, Fisher's exact test). **(c-d)** For longevity, WT recipient animals were treated with a sublethal dose of MITC and then injected with *TBP::mCherry* donor cells. 6-8 weeks after the transplantation, the recipient animals were dissociated, and their mCherry-positive cells were collected by FACS. 40,000 of these were then transplanted again into sublethally MITC-treated recipient animals. 12 transplanted animals and 15 non-transplanted animals (**c**, serial transplantation) were incubated and scored weekly for mCherry signal for 6 weeks **(d)**, representative experiment. The confocal microscope image insets illustrate the mCherry signal in a transplanted animal, 31 days after serial transplantation (d, upper left) and a non-transplanted animal under the same conditions (d, lower right).

Figure 3

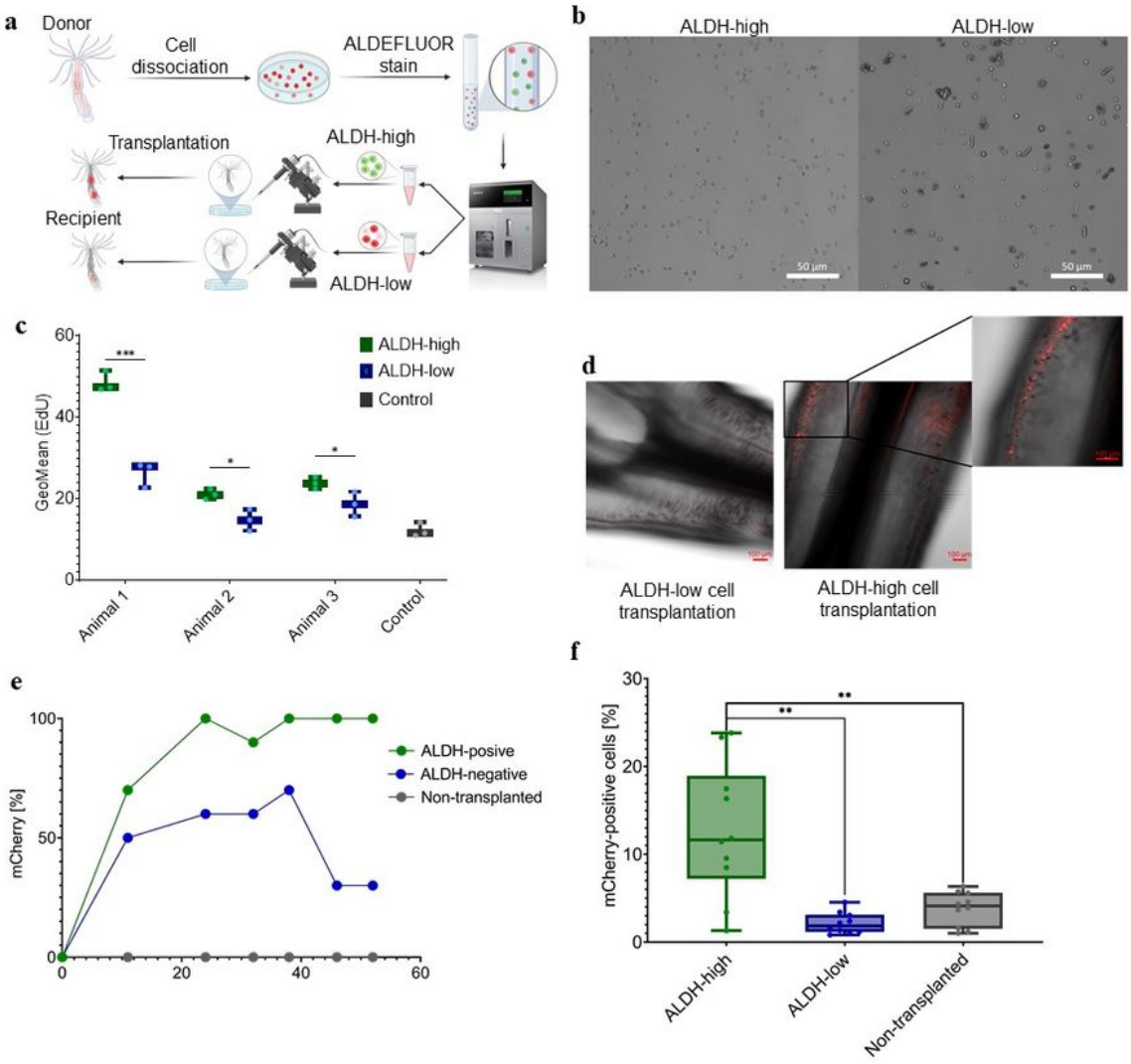

Figure 3

A subpopulation of cells expressing high-ALDH activity with low granularity is enriched for stem cells. (a) Experimentation. Recipient WT animals were treated with a sublethal dose of MITC, 3 days before the transplantation. mCherry-expressing donor animals were dissociated, and the cells were labeled with ALDEFLUOR. FACS was used to isolate an ALDH-high/low granularity (low side-scatter) cell subpopulation and a control ALDH-low/high granularity cell subpopulation. Approximately 10,000 cells of

one subpopulation or other were transplanted into each recipient. **(b)** Images of sorted donor cell subpopulations (ALDH-high, ALDH-low) observed by confocal microscopy. **(c)** For cell proliferation, WT animals were treated with the nucleotide analog EdU for 4 hours. They were then dissociated and sorted, as in (a). Incorporated EdU was quantitated by flow cytometry of triplicate cell subpopulations from each animal (median and minimum to maximum values shown; one-tailed unpaired t-test; Animal 1, P=0.000315; Animal 2, P=0.010042; Animal 3, P=0.02752). **(d)** Confocal microscopy images of recipients were taken 20 days after transplantation of ALDH-high cells (right) or ALDH-low cells (left). **(e)** Representative experiment showing percentage of recipient animals with mCherry signal over time. Recipients were pre-treated with MITC (n=10), ALDH-low (n=10), or Non-transplanted (n=9), accordingly. Then the mCherry signal was assessed by fluorescent microscopy on the indicated days following transplantation. **(f)** Abundance of donor-derived cells in recipients after two months. All recipients were pre-treated with MITC and injected 3 days later with the mCherry-positive donor cell subpopulation indicated, or not injected (non-transplanted). Two months following the transplantation, the recipient animals were dissociated and the fraction of mCherry-positive donor-derived cells measured by flow cytometry. n=10 for each group. (median, 25^{th} to 75^{th} percentiles, and minimum to maximum values shown. ** - P<0.005, Welch's t-test).

Figure 4

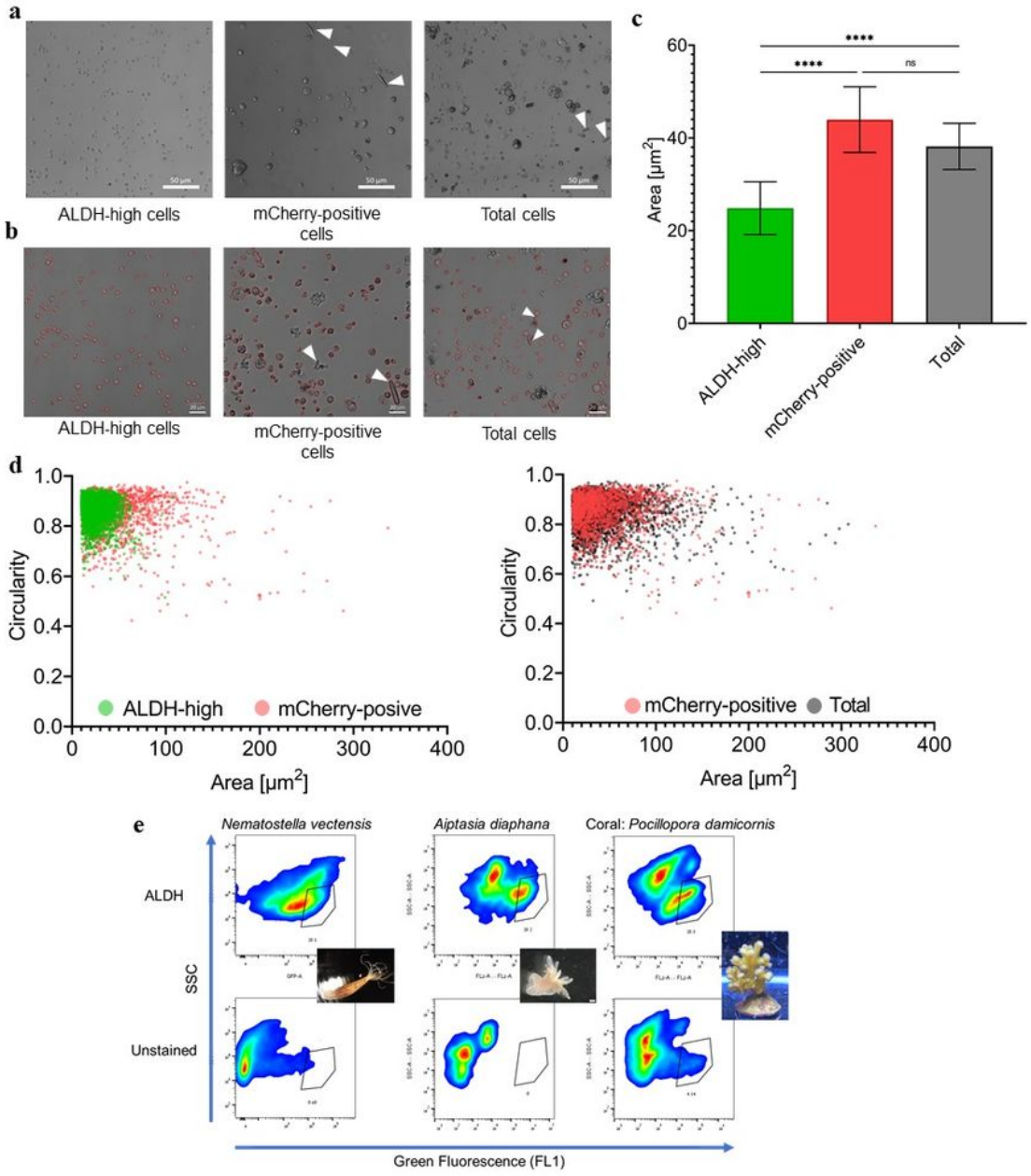

Figure 4

Differentiation of candidate stem cells after transplantation and ALDH as a species non-specific marker. **(a)** Approximately 10,000 donor-derived ALDH-high, mCherry-positive, cells (left) were injected into MITC-treated recipients. Two months after transplantation the recipients were dissociated and donor-derived mCherry-positive cells sorted by FACS (middle). Total recipient cells are also shown (right). Arrows indicate apparent nematocysts (a-b). **(b)** Cell field images from the three cell populations were provided to

a machine learning program that automatically identified cell outlines (in red). **(c-d)** The cell outlines were used by the machine learning algorithm to calculate cell areas **(c)** (n=12 images in mCherry-positive and Total, n=11 images for ALDH-high; Brown-Forsythe and Welch ANOVA tests; ns – P=0.0894; **** - P<0.0001) and circularity. **(d)** Two-dimensional analysis of cell area vs circularity comparing the analyzed cells of mCherry-positive vs the transplanted ALDH (left panel), and vs total cell population (right panel). **(e)** The same flow cytometry gating for the ALDH-high cell population was applied to different hexacorallians; Adult *N. vectensis* (left), *A. diaphna* (middle), and the stony coral *P. damicornis* (right) were either stained for ALDH (upper panels) or not (lower panels) and marked by a gate on the basis of ALDH activity, cell granularity (SSC) and non-specific cell fluorescence (FL1). The identical black gate in each panel indicates a sortable ALDH-high subpopulation in each species.

Supplementary Files

This is a list of supplementary files associated with this preprint. Click to download.

- Taliceetal.Supplementarymaterial.docx